The Effect of Hydrogen on Plasma Nitriding of Austenitic Stainless Steel: Kinetic Modeling

TERESA MOSKALIOVIENE and ARVAIDAS GALDIKAS

The kinetic model of adsorption and stress-induced diffusion of nitrogen in austenitic stainless steels taking place during plasma nitriding using various mixtures of nitrogen and hydrogen is proposed. On the basis of proposed model, a numerical study has been undertaken to analyze and describe the effect of hydrogen on plasma nitriding of austenitic stainless steel. It was shown that the addition of hydrogen with concentrations in the range ~(30 to 40) pct enhances nitrogen penetration into steel. This is due to two factors: (1) reduction of the surface oxide due to chemical etching of the oxygen by hydrogen and (2) increase of NH radicals which are converted to active nitrogen atoms on the steel surface, *i.e.*, the amount of adsorbed and diffused nitrogen increases. As a result, the thicker nitrogen-containing layer is observed. Moreover, results of numerical prediction show that an excessive amount of hydrogen (more than ~70 pct) in the gas mixture retards the nitriding process in comparison with nitriding in pure nitrogen plasma.

DOI: 10.1007/s11661-015-3183-y

I. INTRODUCTION

DESPITE very good corrosion resistance in many aggressive environments, austenitic stainless steels (ASSs) have low hardness and poor tribological properties, which may shorten the life of components, which are subjected to wear.[1,2] Plasma-assisted nitriding of ASS is an excellent method to improve their hardness, wear resistance, and fatigue strength without compromising their well-known corrosion resistance performance.[3–8] Such nitriding processes are performed at moderate temperature, which are necessary to obtain about 10 to 20 μm treatment depths in reasonable times without degradation of corrosion resistance. The moderate [*i.e.*, lower than ~723 K (450 °C)] temperatures suppress the formation of CrN precipitates and the depletion of Cr in the steel matrix, *i.e.*, to prevent a reduction of the corrosion resistance. On the other hand, the lower treatment temperature results in reduced nitriding efficiency compared with higher temperature treatments.[8] Hence, it is very important to enhance the density of active nitriding species in the plasma.

It is known that hydrogen addition to the nitrogen plasma enhances the nitriding rate.[9–18] However, despite the fact, that many experimental studies have analyzed steel surface nitriding processes using nitrogen–hydrogen plasma,[9–18] the role of hydrogen is still not well understood. Overview of literature[9–20] shows that the main and widely stated role of hydrogen on the depth (and also properties) of the nitrided layer is explained by the fact that hydrogen enhances nitrogen diffusion by reducing the diffusion barrier formed by the oxygen adsorbed on the steel surface during nitriding process (oxygen is a common contamination element in plasma chambers, directly affecting the nitriding process[18]) and oxide coverage before the nitriding (natural oxide, whose thickness depends on the pre-history of the sample). For instance, in References 16 through 18, it was established that the chemisorption of oxygen on steel surface diminishes the nitrogen diffusion into the bulk of steel. Hydrogen can be used as a chemical-etching agent to prevent the deleterious effect of oxygen, *i.e.*, to neutralize the effect of the diffusion barrier for nitrogen.[18,19] This process is known as the hydrogen etching mechanism in nitriding process which includes three main steps[18,19]: (1) hydrogen adsorption and dissociation; (2) water molecule formation; and (3) desorption, dragging away water from the steel surface.

Moreover, exhaustive experimental study in Reference 17 proved that hydrogen has an important role on the nitriding process by increasing the density of active nitriding species in the plasma. Similar effect of hydrogen was reported in Reference 21, where it was shown that NH radicals as well as H radicals play an important role in nitriding process. The presence of H radicals may convert NH radical to an active nitrogen atom on the nitride surface more effectively.[21–23] Thus, a kind of catalytic reaction involving the radical species on the steel surface also is responsible for the further enhancement of nitrogen diffusion into the steel bulk.[17,21,22] As a consequence, in order to understand and explain the kinetics of the nitrogen diffusion into the steel bulk, it is necessary to evaluate processes, which take place on the steel surface due to above-mentioned hydrogen actions.

Nitrogen diffusion kinetics is another fundamental challenge. It is well known that nitrogen diffusion in ASS is a complicated process. The nitrogen depth profiles in nitrided ASS exhibit plateau-type shapes, and the behavior of these profiles cannot be explained

TERESA MOSKALIOVIENE, Lecturer, and ARVAIDAS GALDIKAS, Professor, are with the Physics Department, Kaunas University of Technology, Studentų 50, 51368 Kaunas, Lithuania. Contact e-mails: teresa.moskalioviene@ktu.lt, t.moskalioviene@gmail.com

Manuscript submitted May 11, 2015.
Article published online October 1, 2015

by Fick's diffusion equations,[24] even with concentration dependent diffusion coefficient. In our previous works, References 25 through 27 it was shown that internal stress-induced diffusion is responsible for plateau formation in nitrogen depth profile, which is characteristic for nitriding process. The nitrogen concentration gradient and internal stresses gradient are the driving forces of fast (with unusually high diffusion coefficient) nitrogen diffusion. Furthermore, it was found[25] that nitrogen diffusion coefficient in ASS during plasma nitriding vary with nitrogen concentration according to $D(C_N) = f(1/C_N)$. The validity of the stress-induced diffusion model was checked and proved[25–27] for different types of ASS nitrided with different experimental conditions.

The purposes of present work are to analyze the influence of hydrogen on nitriding process and to develop model equations for adsorption, desorption, chemical surface reactions, and diffusion of nitrogen in ASS. For diffusion, the previously developed our model[25–27] is used. The effect of the hydrogen on reducing the oxide layer (that may hinder the nitriding process of steel) and role of NH radicals in order to produce active nitrogen, which then diffuses into the steel and forms the modified layer, are studied by the proposed model.

II. SURFACE INTERACTIONS AND NITROGEN ADSORPTION-DIFFUSION KINETIC MODEL

The plasma with species N_2, H_2, NH, and O_2 is analyzed in order to evaluate the influence of hydrogen. The natural oxide layer with 0.4 μm thickness is taken as the initial condition. Hence, the role of hydrogen is to remove natural oxide layer and to prevent oxidation during nitriding. So, we assume that initially on the surface are Fe and O atoms. At the later stages, *i.e.*, after adsorption, the surface species will be $H_{2(AD)}$, $N_{2(AD)}$, $NH_{(AD)}$, $O_{2(AD)}$, H, O, Fe, and N. The adsorption, desorption, and surface reaction processes occurring on steel surface due to interaction with N_2–H_2 plasma are schematically shown in Figure 1. The process kinetics includes the following steps:

(1) $N_2 + Fe \rightarrow N_{2(AD)}$, $N_{2(AD)} \rightarrow N_{(AD)} + N_{(AD)}$, and $N_{(AD)} \rightarrow N_{DIF}$ describe the adsorption and dissociation of the nitrogen molecule;

(2) $H_2 + Fe \rightarrow H_{2(AD)}$, $H_2 + O \rightarrow H_{2(AD)}$, $H_{2(AD)} \rightarrow H_{(AD)} + H_{(AD)}$, and $H_{(AD)} + H_{(AD)} + O \rightarrow H_2O\uparrow$ describe the adsorption, dissociation of the hydrogen molecule, water formation, and subsequent desorption. The formation and desorption of water cause the oxygen elimination, *i.e.*, a chemical etching of the absorbed oxygen by hydrogen;

(3) $O_2 + Fe \rightarrow O_{2(AD)}$, $O_{2(AD)} \rightarrow O_{(AD)} + O_{(AD)}$, or $O_{2(AD)} \rightarrow O_2\uparrow$ describes the adsorption and dissociation or desorption of the oxygen molecule as oxygen gas;

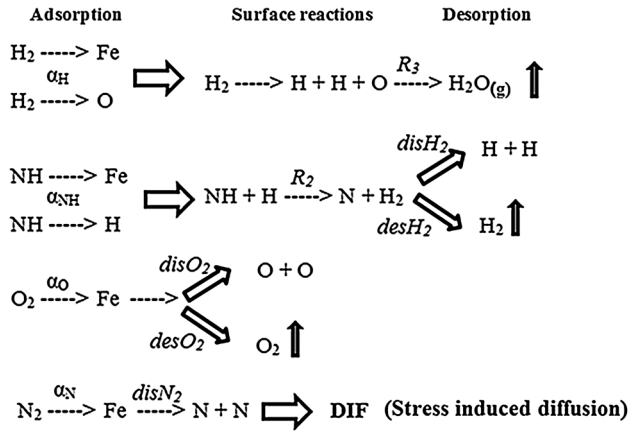

Fig. 1—Schematic representation of plasma species interactions with steel surface.

(4) $NH + Fe \rightarrow NH_{(AD)}$, $NH + H \rightarrow NH_{(AD)}$, $NH_{(AD)} + H_{(AD)} \rightarrow N_{(AD)} + H_{2(AD)}$, $H_{2(AD)} \rightarrow H_2\uparrow$ (or $H_{2(AD)} \rightarrow H_{(AD)} + H_{(AD)}$), and $N_{(AD)} \rightarrow N_{DIF}$, where NH radical is adsorbed on the surface and the collision of adsorbed NH with $H_{(AD)}$ on the steel surface results in the formation of $N_{(AD)}$ and $H_{2(AD)}$ which is converted to H_2 gas and which is desorbed from the surface, while adsorbed nitrogen diffuses into the bulk of steel.

In the present study, penetration of adsorbed nitrogen into the bulk of stainless steel (N_{DIF}), which takes place during plasma nitriding at temperatures below nitrides formation, will be analyzed by stress-induced diffusion model. This model was proposed in our previous works,[25–27] where the influence of internal stresses on nitrogen diffusion is analyzed involving the process of barodiffusion. For solids, pressure gradient is equal to stress gradient $\nabla p = -\nabla\sigma$, and the process is named as stress-induced diffusion. The internal stresses are created by distortion of γ phase alloy lattice by nitrogen atoms. As a result, the γ_N phase is formed with increased lattice parameter. This initiates the swelling process and can change diffusion coefficient. The swelling process and concentration dependent diffusion were analyzed in Reference 25 through 27. It was shown (see Reference 25) that nitrogen diffusion coefficient in steel is concentration dependent and varies with nitrogen concentration according to Einstein–Smoluchowski[28] relation $D(C_N) = f(1/C_N)$. Detailed description of nitrogen diffusion model and the diffusion equations in the presence of internal stresses as driving force of diffusion are presented in References 25 through 27.

Taking to account the above listed interactions and mass transport processes, the rate equations can be presented as follows:

for steel surface layer ($k = 0$),

$$\begin{cases} \dfrac{dC_{H_2}}{dt} = \alpha_H \cdot i_{H_2} \cdot \left(C_{Fe}^{(k)} + C_O^{(k)}\right) - dis_{H_2} \cdot C_{H_2} + \dfrac{1}{2} \cdot R_2 \cdot C_{NH} \cdot C_H - des_{H_2} \cdot C_{H_2} \\ \dfrac{dC_H}{dt} = 2 \cdot dis_{H_2} \cdot C_{H_2} - \dfrac{1}{2} \cdot R_3 \cdot C_O \cdot (C_H)^2 - \alpha_{NH} \cdot i_{NH} \cdot C_H \\ \dfrac{dC_{NH}}{dt} = \alpha_{NH} \cdot i_{NH} \cdot \left(C_H + C_{Fe}^{(k)}\right) - R_2 \cdot C_{NH} \cdot C_H \\ \dfrac{dC_{O_2}}{dt} = \alpha_O \cdot i_{O_2} \cdot C_{Fe}^{(k)} - dis_{O_2} \cdot C_{O_2} - des_{O_2} \cdot C_{O_2} \\ \dfrac{dC_O^{(k)}}{dt} = 2 \cdot dis_{O_2} \cdot C_{O_2} - \alpha_H \cdot i_{H_2} \cdot C_O^{(k)} - \dfrac{1}{2} \cdot R_3 \cdot C_O^{(k)} \cdot (C_H)^2 + \dfrac{D_O}{h^2} \cdot \left(C_O^{(k+1)} - C_O^{(k)}\right) \\ \dfrac{dC_{N_2}}{dt} = \alpha_N \cdot i_{N_2} \cdot C_{Fe}^{(k)} - dis_{N_2} \cdot C_{N_2} \\ \dfrac{dC_{Fe}^{(k)}}{dt} = -2 \cdot dis_{O_2} \cdot C_{O_2} + des_{H_2} \cdot C_{H_2} + des_{O_2} \cdot C_{O_2} + R_3 \cdot C_O^{(k)} \cdot (C_H)^2 \\ \qquad - \alpha_O \cdot i_{O_2} \cdot C_{Fe}^{(k)} - \alpha_H \cdot i_{H_2} \cdot C_{Fe}^{(k)} - \alpha_{NH} \cdot i_{NH} \cdot C_{Fe}^{(k)} - \alpha_N \cdot i_{N_2} \cdot C_{Fe}^{(k)} + \dfrac{D_{Fe}}{h^2} \cdot \left(C_{Fe}^{(k+1)} - C_{Fe}^{(k)}\right) \\ \dfrac{dC_N^{(k)}}{dt} = 2 \cdot dis_{N_2} \cdot C_{N_2} + \dfrac{1}{2} \cdot R_2 \cdot C_{NH} \cdot C_H + DIF_N^{(k)} \end{cases} \quad [1]$$

and for other steel layers ($k > 0$)

$$\begin{cases} \dfrac{dC_{Fe}^{(k)}}{dt} = \dfrac{D_{Fe}}{h^2} \cdot \left(C_{Fe}^{(k+1)} + C_{Fe}^{(k-1)} - 2 \cdot C_{Fe}^{(k)}\right) \\ \dfrac{dC_O^{(k)}}{dt} = \dfrac{D_O}{h^2} \cdot \left(C_O^{(k+1)} + C_O^{(k-1)} - 2 \cdot C_O^{(k)}\right) \cdot \\ \dfrac{dC_N^{(k)}}{dt} = DIF_N^{(k)} \end{cases} \quad [2]$$

The term DIF_N is the diffusion term, which describes the process of nitrogen concentration dependent diffusion in the presence of internal stresses as driving force of diffusion[25–27]:

$$DIF_N = \frac{\partial D(C_N)}{\partial C_N(x,t)} \nabla_x C_N(x,t) \nabla_x C_N(x,t) + D(C_N) \nabla_x^2 C_N(x,t) - \frac{V_N}{RT} \begin{pmatrix} C_N(x,t) \dfrac{\partial D(C_N)}{\partial C_N(x,t)} \nabla_x C_N(x,t) \nabla_x \sigma(x,t) \\ + D(C_N) \nabla_x C_N(x,t) \nabla_x \sigma(x,t) \\ + D(C_N) C_N(x,t) \nabla_x^2 \sigma(x,t) \end{pmatrix}; \quad [3]$$

where $D = D_{const}/C_N$; $\sigma = -X_{stress} \cdot C_N$.[25–27]

The C_{H_2}, C_H, C_{NH}, C_{O_2}, C_O, C_{N_2}, C_{Fe}, and C_N are relative concentrations of H_2, H, NH, O_2, O, N_2, Fe, and N, respectively; α_{NH}, α_O, α_H, and α_N are the sticking coefficients of NH radical, O_2, H_2, and N_2 to the corresponding steel surface components (possible adsorption sites were defined above); i_N is relative flux of nth component to the surface; $R_{2,3}$ are the reaction rate constants; des_N and dis_N are desorption and dissociation probabilities of nth component, respectively; h is the thickness of layer; D is diffusion coefficient; σ is a compositionally induced internal stress; X_{stress} is the proportionality constant (in MPa·/(at. pct)); and D_{const} is the phenomenological diffusion constant of nitrogen independent on nitrogen concentration.

The developed kinetic model equations (Eqs. [1] through [3]) were solved using finite difference method, and for the numerical calculations, a computer program was created using C++ programming code and C++ Builder software package.

III. RESULTS AND DISCUSSION

In order to analyze the role of hydrogen on nitriding process of austenitic stainless steel in nitrogen–hydrogen gas mixture plasma, AISI 316L steel (11.27 at. pct Ni, 18.66 at. pct Cr, 1.71 at. pct Mn, 0.61 at. pct Si, 1.3 at. pct Mo, balance Fe) is selected as the base material for calculations. Values of model parameters V_N, N_0, and X_{stress} for this material (AISI 316L steel) were taken from literature: $V_N = 3.9 \times 10^{-5}$ m^3 mol^{-1}[29]; the proportionality constant $X_{stress} = 200$ MPa (at. pct)$^{-1}$[30]; $N_0 = 0.81 \times 10^{23}$ cm^{-3}.[25] The values of all other model parameters related with adsorption/desorption process were defined from literature data and are listed in Table I. The values of adsorption, desorption, and dissociation probabilities (in Table I) have been estimated according to adsorption, desorption, and dissociation activation energy values, which were taken from the literature[31–40] for corresponding component. To analyze the influence of hydrogen as absolute quantity and relative quantity, the calculations were performed in two stages: (1) when the proportion of hydrogen was varied while the total flux of nitrogen–hydrogen gas mixture was kept as a constant

Table I. Simulation Parameters

α_O	0.5	dis_{H_2} (s^{-1})	0.6
α_{NH}	0.1	dis_{N_2} (s^{-1})	0.4
α_H	0.2	dis_{O_2} (s^{-1})	0.7
α_N	0.2	R_2 (s^{-1})	0.5
des_{O_2} (s^{-1})	0.2	R_3 (s^{-1})	0.5
des_{H_2} (s^{-1})	0.3	D_O ($cm^2\ s^{-1}$)	1×10^{-10}[39]
i_N (s^{-1})	9.3×10^{-4}	D_{Fe} ($cm^2\ s^{-1}$)	1×10^{-14}[40]
i_O (s^{-1})	1.9×10^{-6}	D_{const} ($cm^2\ s^{-1}$)	8.2×10^{-13}[27]

Mechanical Properties of AISI 316L (DIN 1.4404-X2CrNiMo1712 2)

Yield Strength $Rp_{0.2}$ (MPa)	Tensile Strength R_m (MPa)	Percent Elongation (Pct)	Vickers Hardness (HV)
170	485	40	200 to 210

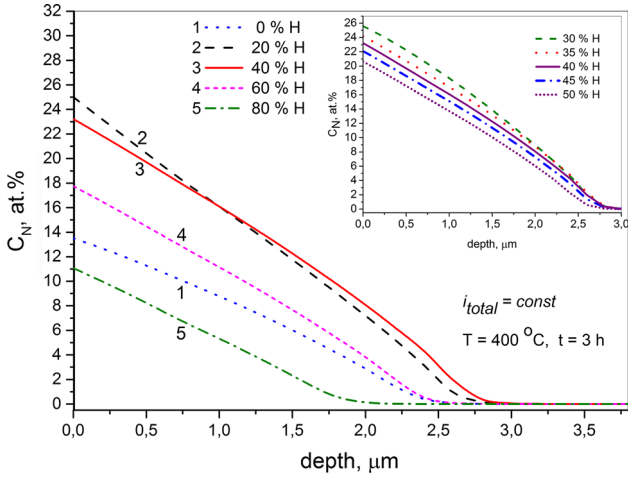

Fig. 2—Calculated nitrogen depth profiles after plasma nitriding of austenitic stainless steel AISI 316L at 673 K (400 °C) for 3 h with the different percentage of hydrogen in the nitrogen–hydrogen mixture when the total flux of N_2–H_2 mixture was kept as a constant, while the proportion of hydrogen was varied.

($i_N + i_H = 9.3 \times 10^{-4}\ s^{-1}$) and (2) when a relative flux of nitrogen was held constant ($i_N = 9.3 \times 10^{-4}\ s^{-1}$), so that the total flux of N_2–H_2 mixture was increased by the addition of hydrogen.

The nitrogen concentration depth profiles calculated by the model Eqs. [1] through [3] after plasma nitriding of austenitic stainless steel AISI 316L at 673 K (400 °C) for 3 hours are shown in Figure 2. Five curves represent different percentages of hydrogen in the nitrogen–hydrogen mixture (note that the total flux of N_2–H_2 mixture was kept as a constant, while the proportion of hydrogen was varied). The results show that with the increase of the ratio of hydrogen in total mixture flux to ~40 pct, the surface concentration and the penetration depth of nitrogen increase. However, a further increase of hydrogen amount (more than 40 pct) in the gas mixture decelerates the nitriding process. Curves 4 and 5 in Figure 2 calculated at 60 and 80 pct of hydrogen show lower penetration depth of nitrogen. However, hydrogen does not directly influence diffusivity of nitrogen. With the increase of hydrogen, the amount of nitrogen decreases and, as a result, thickness of nitrided layer decreases. The results presented in Figure 2 suggest that the presence of hydrogen in the gas mixture of plasma has several effects. The first one is that hydrogen reduces the surface oxide layer. Figure 3 shows the calculated oxygen depth profiles in steel nitrided with the different percentages of hydrogen in the N_2–H_2 mixture. Considering Reference 41, the steel surfaces exhibit an oxide coverage before the nitriding which depends on the pre-history of the sample. After starting the nitriding, the oxygen content of the surface is reduced due to hydrogen etching mechanism. So, as the initial condition for calculations, the natural oxide layer of 0.4 μm thickness is taken (see Figure 3, the curve of the initial profile). As it can be seen in Figure 3, the increase of hydrogen ratio in total incident flux leads to decrease in oxygen concentration on the surface and correspondingly to the decrease of the total amount of oxygen in steel. The shape of the oxygen concentration profiles is determined by the oxygen diffusion into the steel bulk and toward steel surface, where it is removed by the hydrogen assistance. Figures 4 and 5 demonstrate the correlation between the removal of the surface oxide and the nitrogen penetration into the bulk. Figure 4 shows the evolution of the nitrogen and oxygen concentrations on the surface as a function of the percentage of hydrogen in the nitrogen–hydrogen mixture. The results show (see Figure 4, curves 1 and 2) that hydrogen diminishes the absorbed oxygen content while augmenting the nitrogen concentration at the steel surface. Then it contributes to higher nitrogen content available for the diffusion into the steel bulk and, as result, the thicker nitrogen-containing layers in a given treatment time and temperature are observed. This is clearly seen in Figure 5(see curve 1) where the variation of nitrogen penetration depth (or the thickness of the modified layer) as a function of hydrogen percentage in the nitriding plasma is shown. As a penetration depth, we are assuming distance from the surface until layer with nitrogen relative concentration equal to about 2 at. pct.

The next important effect is that hydrogen, as the gas in the nitriding process contributes to the production of nitrogen atoms on steel surface *via* NH radicals.[17,21] Several studies[21–23] report results of plasma diagnostics (optical emission spectroscopy) of the nitrogen–hydrogen

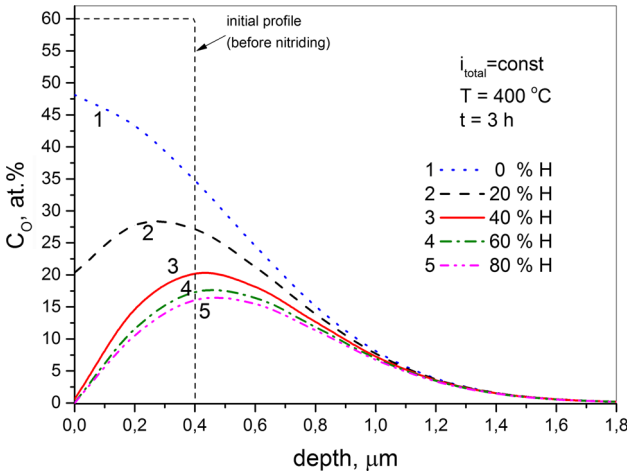

Fig. 3—Calculated oxygen depth profiles in plasma nitrided AISI 316L at 673 K (400 °C) for 3 h with the different percentage of hydrogen in the nitrogen–hydrogen mixture (the total flux of N_2–H_2 mixture was kept as a constant, while the proportion of hydrogen was varied).

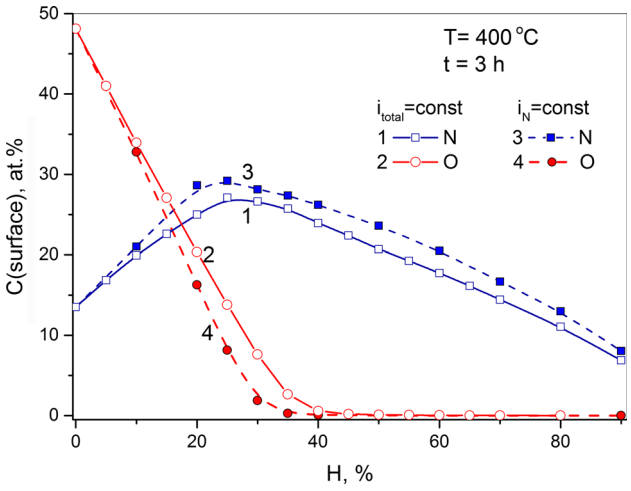

Fig. 4—The evolution of the nitrogen and oxygen concentrations on steel surface as a function of the percentage of hydrogen in the nitrogen–hydrogen mixture (curves 1 and 2—when the total flux of N_2–H_2 mixture was kept as a constant; curves 3 and 4—when relative flux of nitrogen was held constant).

plasma with various proportions of hydrogen, and there is general agreement that the concentrations of N_2 and nitrogen molecular ions, N atoms, and nitrogen atomic ions decrease with increasing hydrogen ratio above 20 pct, while the maximum content of NH radicals is observed at 20 to 40 pct of H_2 (for example see Figure 8 in Reference 21). Thus ,for the calculations, it is important to define the relative flux of NH radicals which is dependent on the ratio of hydrogen to nitrogen in gas mixture. This dependence has been qualitatively and quantitatively determined according to results from References 21, 23 (see Figure 8 in Reference 21 and Figure 9 in Reference 23:

for $P = 0$ and 85 pct $< P \le 100$ pct:

$$i_{NH} = 0;$$

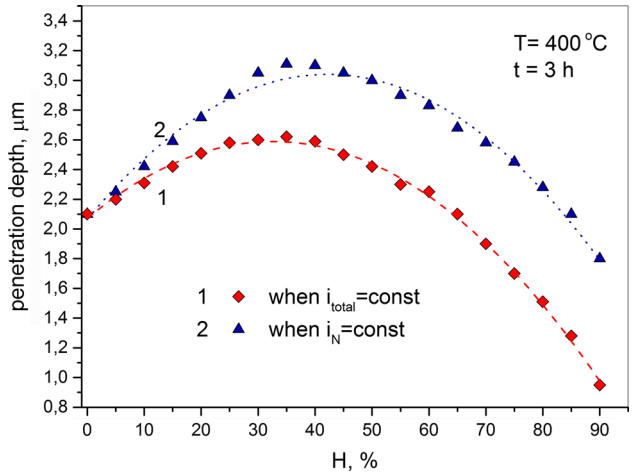

Fig. 5—The variation of nitrogen penetration depth (or modified layer thickness) as a function of percentage hydrogen in the nitriding plasma (curve 1—when the total flux of N_2–H_2 mixture was kept as a constant; curve 2—when relative flux of nitrogen was held constant). As a penetration depth, we are assuming distance from the surface until layer with nitrogen relative concentration equal to about 2 at. pct.

for 0 pct $< P \le 40$ pct:

$$i_{NH} \cong 2 \times 10^{-9} \cdot (P)^3 - 2 \times 10^{-7} (P)^2 + 1 \times 10^{-5} (P)^1 - 2 \times 10^{-6};$$

for 40 pct $< P \le 85$ pct:

$$i_{NH} \cong 3 \times 10^{-8} \times (P)^2 - 7 \times 10^{-6} (P)^1 + 0.0003,$$

where P is the percentage of hydrogen in the nitrogen hydrogen mixture (in at. pct, P = at. pct H_2).

Hereby, the increase of the surface concentration and the penetration depth of nitrogen with the increase of the ratio of hydrogen in total mixture flux (to ~40 pct) is due to two factors: (1) the chemical etching of surface oxide by hydrogen and (2) increase of NH radicals which are converted to an active nitrogen atoms on the steel surface and can then diffuse into the bulk. With the increase of hydrogen amount in total mixture flux more than 40 pct, the surface concentration of nitrogen and the modified layer thickness decrease (Figure 5). It can be explained by the fact, that with increase of hydrogen percentage in total mixture flux, the nitrogen amount decreases accordingly (in the case when total flux of mixture is kept as a constant), *i.e.*, it contributes to lower nitrogen content on steel surface available for the diffusion into the steel bulk. Moreover, as it was mentioned above, if hydrogen content exceeds 40 pct, the amount of NH radicals also reduces, so that the adsorbed nitrogen content decreases and, as a result, the thinner nitrogen-containing layer is observed.

Figure 6(a) shows the calculated nitrogen depth profiles after plasma nitriding with the different percentage of hydrogen in the N_2–H_2 mixture when relative flux of nitrogen was kept as constant (i_N = const). So, in this case the total flux of N_2–H_2 mixture was increased by the addition of hydrogen ($i_H = \frac{i_N \cdot (P)}{100\,\text{pct} - (P)}$, P is the percentage

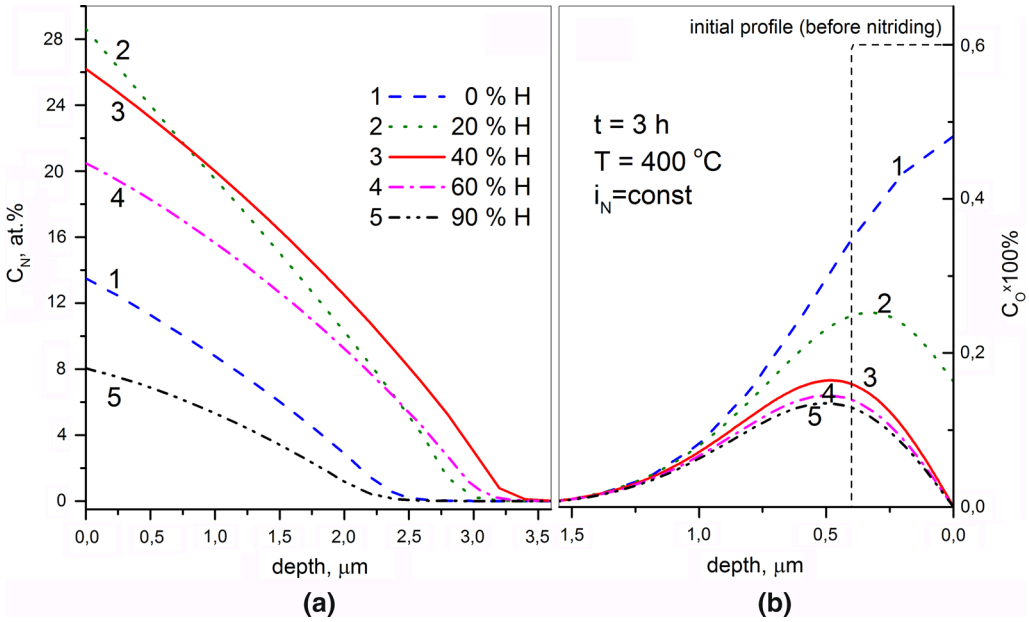

Fig. 6—The calculated (*a*) nitrogen depth profiles and (*b*) oxygen depth profiles after plasma nitriding of AISI 316L at 673 K (400 °C) for 3 h with the different percentage of hydrogen in the nitrogen–hydrogen mixture when relative flux of nitrogen was held constant (i_N = const).

of hydrogen in the mixture). The results of Figure 6(a) show that optimal amount of hydrogen, which gives optimum modified layer thickness and total concentration of nitrogen in steel in a given treatment time and temperature is about 40 pct. As it can be seen in Figures 4 through 6(b) (see curves for i_N = const) with increase of hydrogen amount up to approximately 30 to 40 pct, the removing process of oxygen from the steel surface is enhanced and reaches a maximum. As a result, the amount of adsorbed and diffused nitrogen increases. Furthermore, according to previous analysis, the amount of NH radicals also rises, so that the adsorbed nitrogen content increases. A further increase of hydrogen amount (more than 40 pct) in the gas mixture decelerates the nitriding process because of amount of nitrogen and NH radicals in the nitriding plasma fall with the addition of hydrogen. Thus, more adsorption sites are occupied by hydrogen, and as a result, the amount of adsorbed nitrogen decreases; consequently, the surface concentration and the penetration depth of nitrogen decrease. Obtained modeling results are in agreement with experimental results presented in References 16, 21. For example, experimental results from Reference 16 were reproduced in Figure 7. As it can be seen in Figure 7 the modified layer thickness (see Figure 7(a)) and microhardness (see Figure 7(b)) of AISI 316 stainless steel samples nitrided at 673 K (400 °C) reach maximum at 20 to 40 pct of hydrogen (when flux of nitrogen is maintained). Moreover, the addition of hydrogen more than about 40 to 50 pct to nitrogen plasma results in decrease of nitriding efficiency.

The variation of nitrogen penetration depth as a function of the hydrogen percentage in the nitriding plasma when the proportion of hydrogen was varied while i_{total} = const and when i_N = const are qualitatively comparable (see Figure 5). Quantitative distinctions are due to different relative fluxes of nitrogen in these two cases. As it can be seen in Figure 5, the modified layer thickness is about 2.1 μm for these two cases (curve 1 for i_{total} = const and curve 2 for i_N = const) when there are no hydrogen in plasma because of the same initial values of nitrogen flux. The penetration depth of nitrogen increases as the content of hydrogen is increased from 0 to 40 pct. However, once the content of hydrogen is increased more than 40 pct, there is a significant drop in the concentration and penetration depth of nitrogen in the sample.

The process kinetics is analyzed in Figures 8 and 9. The calculated nitrogen and oxygen depth profiles at different moments of nitriding time (40 at. pct H_2) are plotted in Figure 8. The results show that at the beginning, the oxygen content at the surface is reduced by hydrogen. Oxygen diffuses towards the surface and bulk according formed gradients. An increase of nitrogen surface concentration corresponds to a decrease of oxygen content on the surface. Thus as a result, the thickness of the modified layer increases with nitriding time. The time dependences of nitrogen and oxygen surface concentration at different contents of hydrogen in the N_2–H_2 mixture are presented in Figure 9. The nitrogen surface concentration increases rapidly at the initial stages of nitriding processes and later slowly approaches steady state value. The steady state at the surface has been reached after a process time which depends on the content of hydrogen in the incoming N_2–H_2 flux. After a stationary state at the surface has been achieved, the nitriding process becomes diffusion controlled. Higher content of hydrogen in incoming gas mixture reduces time needed to reach a steady state of nitrogen surface concentration (see Figure 9). However,

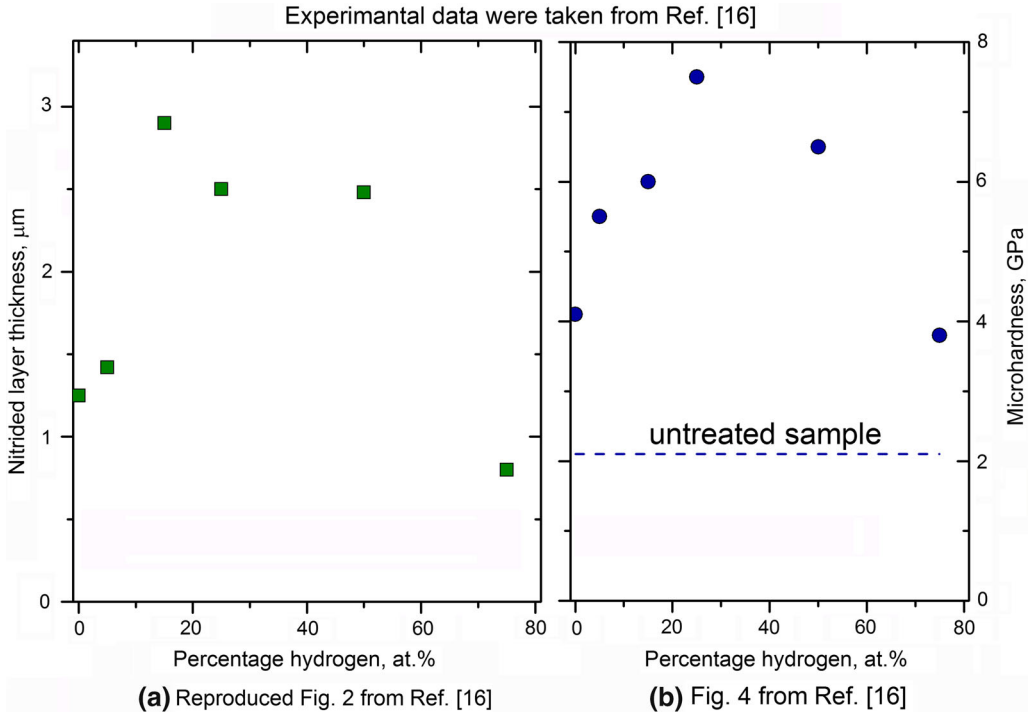

Fig. 7—The variation (*a*) in the thickness of the modified layer and (*b*) of microhardness of AISI 316 nitrided for 3 h at 673 K (400 °C) with the percentage of hydrogen in the gas mixture. Data were taken from Ref. [16].

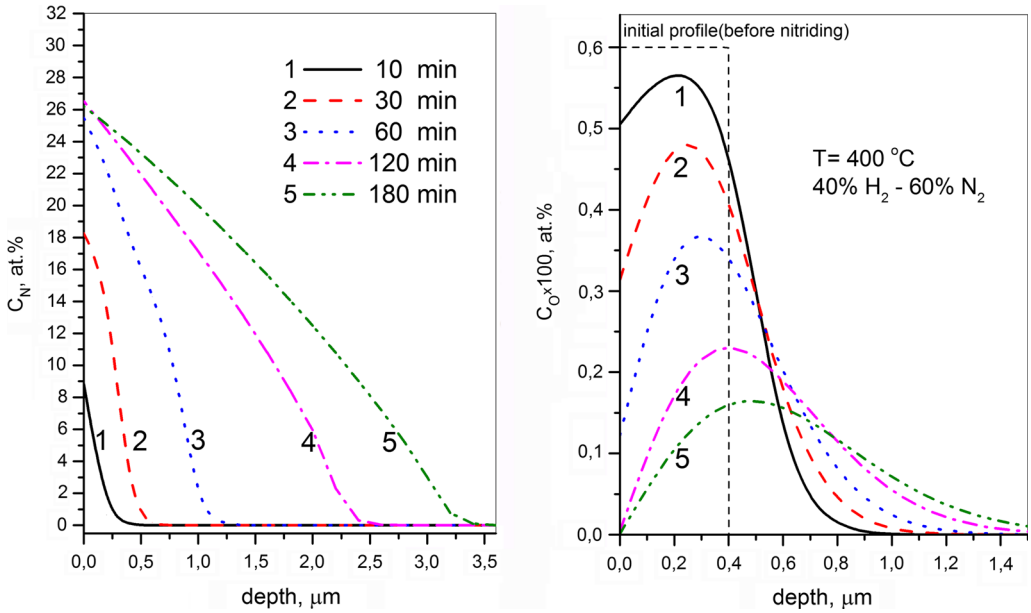

Fig. 8—Time evolution of the calculated nitrogen and oxygen profiles in nitrided AISI 316L at T = 673 K (400 °C) and 40 at. pct H_2.

with the increase of hydrogen amount more than 40 pct, more adsorption sites are occupied by hydrogen and as a result amount of adsorbed nitrogen decreases.

IV. CONCLUSIONS

In the present work, a kinetic nitrogen adsorption and diffusion model is proposed to describe and analyze the effect of hydrogen on plasma nitriding of austenitic stainless steel. According to the theoretical analysis, the addition of hydrogen with concentrations in the range ~(30 to 40) pct enhanced nitrogen penetration into steel, and the nitriding is more efficient than with pure nitrogen plasma, by allowing a thicker modified layer and higher nitrogen content in the steel. It was shown that with increase in the amount of hydrogen to ~40 pct, the removing process of oxygen from the steel surface is enhanced and reaches a maximum, *i.e.*, the amount of adsorbed and diffused nitrogen increases. Furthermore,

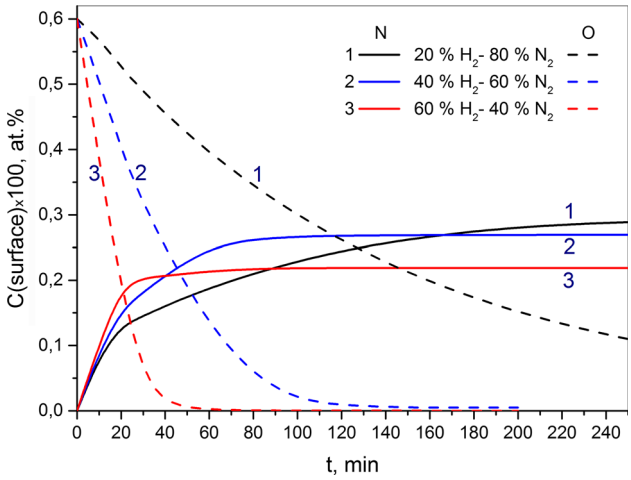

Fig. 9—The dependence of nitrogen and oxygen surface concentration on nitriding duration at different content of hydrogen in the nitrogen–hydrogen mixture.

the presented model considered the presence of NH radicals which are converted to active nitrogen atoms on the steel surface and then diffuse into the steel bulk, and as a result, the thicker nitrogen-containing layer is observed. Finally, prediction results show that an excessive amount of hydrogen (more than ~70 pct) in the gas mixture retards the nitriding process in comparison with nitriding in pure nitrogen plasma.

ACKNOWLEDGMENT

This research was funded by a Grant (No. MIP-030/2013) from the Research Council of Lithuania.

REFERENCES

1. V. Singh, K. Marchev, C.V. Cooper, and E.I. Meletis: *Surf. Coat. Technol.*, 2002, vol. 160, p. 249.
2. S. Picard, J.B. Memet, R. Sabot, J.L. Grosseau-Poussard, J.P. Rivière, and R. Meilland: *Mater. Sci. Eng. A*, 2001, vol. 303, pp. 163–72.
3. E. Menthe and K.-T. Rie: *Surf. Coat. Technol.*, 1999, vols. 116–119, pp. 199–204.
4. Y. Zhao, B. Yu, L. Dong, H. Du, and J. Xiao: *Surf. Coat. Technol.*, 2012, vol. 210, pp. 90–96.
5. J.M. Priest, M.J. Baldwin, M.P. Fewell, S.C. Haydon, G.A. Collins, K.T. Short, and J. Tendys: *Thin Solid Films*, 1999, vol. 345, pp. 113–18.
6. S. Mändl, B. Fritzsche, D. Manova, D. Hirsch, H. Neumann, E. Richter, and B. Rauschenbach: *Surf. Coat. Technol.*, 2005, vol. 195, pp. 258–63.
7. T. Czerwiec, H. Michel, and E. Bergmann: *Surf. Coat. Technol.*, 1998, vols. 108–109, pp. 182–90.
8. T. Czerwiec, N. Renevier, and H. Michel: *Surf. Coat. Technol.*, 2000, vol. 131, pp. 267–77.
9. G.G. Tibbets: *J. Appl. Phys.*, 1974, vol. 45, pp. 5072–73.
10. A. Szasz, D.J. Fabian, A. Henry, and Z. Szaszne-Csih: *J. Appl. Phys.*, 1989, vol. 66, pp. 5598–5601.
11. J. Bougdira, G. Henrion, and M. Fabry: *J. Phys. D Appl. Phys.*, 1991, vol. 24, pp. 1076–80.
12. M. Hudis: *J. Appl. Phys.*, 1972, vol. 44, pp. 1489–96.
13. D. Hovorka, J. Vlček, R. Čerstvý, J. Musil, P. Bělský, M. Ružička, and J.G. Han: *J. Vac. Sci. Technol. A*, 2000, vol. 18, p. 2715.
14. A. Garamoon, U.M. Rashed, A. Abouelela, M.A. Eissa, A.H. Saudi, D.M. El-zeer, and F. El-Hossary: *IEEE Trans. Plasma Sci.*, 2006, vol. 34, pp. 1066–73.
15. L. Wang, X. Xu, Z. Yu, and Z. Hei: *Surf. Coat. Technol.*, 2000, vol. 124, pp. 93–96.
16. S. Kumar, M.J. Baldwin, M.P. Fewell, S.C. Haydon, K.T. Short, G.A. Collins, and J. Tendys: *Surf. Coat. Technol.*, 2000, vol. 123, pp. 29–35.
17. J.M. Priest, M.J. Baldwin, and M.P. Fewell: *Surf. Coat. Technol.*, 2001, vol. 145, pp. 152–63.
18. C.A. Figueroa, D. Wisnivesky, and F. Alvarez: *J. Appl. Phys.*, 2002, vol. 92, p. 764.
19. C.A. Figueroa and F. Alvarez: *J. Vac. Sci. Technol. A*, 2005, vol. 23, p. L9.
20. C.A. Figueroa, S. Weber, T. Czerwiec, and F. Alvarez: *Scripta Mater.*, 2006, vol. 54, pp. 1335–38.
21. M. Tamaki, Y. Tomii, and N. Yamamoto: *Plasmas Ions*, 2000, vol. 3, pp. 33–39.
22. L. Petitjean and A. Ricard: *J. Phys. D Appl. Phys.*, 1984, vol. 17, pp. 919–29.
23. H. Martınez and F.B. Yousif: *Eur. Phys. J. D*, 2008, vol. 46, pp. 493–98.
24. S. Parascandola, W. Moller, and D.L. Williamson: *Appl. Phys. Lett.*, 2000, vol. 76, pp. 2194–96.
25. T. Moskalioviene and A. Galdikas: *Vacuum*, 2012, vol. 86, pp. 1552–57.
26. A. Galdikas and T. Moskalioviene: *Surf. Coat. Technol.*, 2011, vol. 205, pp. 3742–46.
27. A. Galdikas and T. Moskalioviene: *Comput. Mater. Sci.*, 2013, vol. 72, pp. 140–45.
28. A. Einstein: *Ann. Phys.*, 1905, vol. 17, pp. 549–60.
29. S. Jegou, L. Barrallier, and R. Kubler: *Acta Mater.*, 2010, vol. 58, pp. 2666–76.
30. T. Christiansen and M. Somers: *Mater. Sci. Eng. A*, 2006, vol. 424, pp. 181–89.
31. G. Ertl and M. Huber: *Z. Phys. Chem. N. F.*, 1980, vol. 119, pp. 97–102.
32. M. Weiss, G. Ertl, and F. Nitschké: *Appl. Surf. Sci.*, 1979, vol. 2, pp. 614–35.
33. Ch.H. Shon and T. Makabe: *IEEE Trans. Plasma Sci.*, 2004, vol. 32, pp. 390–97.
34. E.A. Kurz and J.B. Hudson: Technical Report No. 4 Contract N00014-86-K-0259, 1988.
35. I. Goikoetxea, M. Alducin, R. Dıez Muino, and J.I. Juaristi: *Phys. Chem. Chem. Phys.*, 2012, vol. 14, pp. 7471–80.
36. B. Darwen: U.S. National Bureau of Standards, 1970.
37. Sh. Zhang and T.N. Truong: *J. Chem. Phys.*, 2000, vol. 113, p. 6149.
38. I. John Prigogine: *Advances in Chemical Physics*, Wiley, New York, 2009, pp. 8–539.
39. J. Takada, S. Yamamoto, Sh. Kikuchi, and M. Adachi: *Metall. Trans. A*, 1986, vol. 17A, pp. 221–29.
40. K. Takeda, K. Yamashita, Y. Murata, T. Koyama, and M. Morinaga: *Mater. Trans.*, 2008, vol. 49, pp. 479–83.
41. W. Möller, S. Parascandola, T. Telbizova, R. Günzel, and E. Richter: *Surf. Coat. Technol.*, 2001, vol. 136, pp. 73–79.